Materials Science-Poland, *Vol. 27*, *No. 3*, *2009*

High temperature impedance spectroscopy study of non-stoichiometric bismuth zinc niobate pyrochlore

K. B. TAN[1*], C. C. KHAW[2], C. K. LEE[3], Z. ZAINAL[1], Y. P. TAN[1], H. SHAARI[1]

[1]Faculty of Science, Universiti Putra Malaysia, 43400 Serdang, Selangor, Malaysia

[2]Faculty of Engineering and Science, Universiti Tunku Abdul Rahman, 53300 Kuala Lumpur, Malaysia

[3]Academic Science Malaysia, 902-4 Jalan Tun Ismail, 50480 Kuala Lumpur, Malaysia

Single phase non-stoichiometric bismuth zinc niobate, $Bi_3Zn_{1.84}Nb_3O_{13.84}$, was fabricated by a conventional solid state method. The sample was refined and fully indexed on the cubic system, space group *Fd*3*m* (No. 227), $Z = 4$ with $a = 10.5579(4)$ Å. Electrical characterisation was performed using an ac impedance analyser over the temperature range of 25–850 °C and frequency range of 5 Hz–13 MHz. Typical dielectric response is observed in $Bi_3Zn_{1.84}Nb_3O_{13.84}$ with a high relative permittivity, low dielectric loss and a negative temperature coefficient of capacitance, with the values of 147, 0.002 and –396 ppm/°C, at 100 kHz at ambient temperature, respectively. This material is highly resistive, with a conductivity of 1×10^{-21} $\Omega^{-1}\cdot cm^{-1}$ and a high activation energy of ca. 1.59 eV.

Key words: *activation energy; bismuth zinc niobate; dielectric response; impedance spectroscopy; pyrochlore*

1. Introduction

Ceramic materials have been used in a wide range of industrial applications such as electrical and electronic components, superconductors, catalyst and automobile components [1–3]. The study of advanced ceramic materials involves many disciplines, including chemistry, physics, mechanical engineering, materials science and metallurgy. Both electroceramics and structural ceramics are classified as advanced ceramics, and they have different applications. Applications of electroceramics involve electrical and magnetic properties, whereas those of structural ceramics are mainly based on its mechanical behaviour [4].

One of the promising candidates in electroceramics is bismuth pyrochlore [5]. Pure bismuth oxides are highly reactive, volatile and thermally unstable with poly-

*Corresponding author, e-mail: tankb@science.upm.edu.my

morphic transitions in which monoclinic α-Bi_2O_3 transforms to a defect fluorite δ-Bi_2O_3 above 729 °C, and then followed by the formation of two metastable phases, tetragonal β-Bi_2O_3 and body-centred cubic γ-Bi_2O_3 upon cooling [6]. However, bismuth derivatives are suitable and cost effective for various commercial applications, particularly in microwave and radio frequency applications, due to their low firing temperatures of miniaturisation with passive integration using multilayer ceramic technology whereby active or passive components are laminated and co-fired at low temperature. In general, pyrochlore materials have the formula, $A_2B_2O_7$ indicating the existence of two different crystallographic sites, namely a relatively larger 8-coordinate A site and a smaller 6-coordinate B site within the structure. These sites are commonly occupied by a combination of A^{3+} and B^{4+} cations, A^{2+} and B^{5+} cations or other combinations with required average mixed valency [7]. By far the most extensively studied Bi-based dielectrics are the cubic pyrochlore $Bi_{3/2}ZnNb_{3/2}O_7$ ($k' = 150$, $t_k = -400$ ppm/°C) and the monoclinic zirconolite phase ($k' = 80$, $t_k = 200$ ppm/°C, k' is the relative electric permittivity, and t_k stands for the temperature coefficient of capacitance). With the opposite signs for the temperature dependence of permittivity, they are considered a good pair that provides temperature compensated dielectric properties when mixed together [8].

An "ideal" composition for a pyrochlore phase in the Bi_2O_3–ZnO–Nb_2O_5 (BZN) system could be $Bi_3Zn_2Nb_3O_{14}$, referred to as P, in which the expectation is that part of Zn and all Bi would be disordered over the large, 8-coordinate A sites; the remainder of Zn, together with Nb, would be disordered over the octahedral B sites. However, it has been shown that the material of the composition $Bi_3Zn_2Nb_3O_{14}$ contains excessive ZnO as a second phase and lies outside the BZN subsolidus solid solution area [9–13]. The pure-phase composition was confirmed to be ZnO deficient by electron probe microanalysis and a combination study of electron, neutron and X-ray diffraction.

Work since the 1990's has clarified many of the fundamental aspects of BZN materials. However, there are inconsistencies and discrepancies in the literature regarding the characterization of BZN materials. In particular, estimates of the electric relative permittivities, as reported from different researchers working on multiphase samples, can vary anywhere in the 80–120 range [9–13]. Preliminary electrical studies on Bi_2O_3–ZnO–Nb_2O_5 ternary system indicate that these materials are highly insulating and their conductivities are not likely to be determined at temperatures below 500 °C. However, it is possible to measure permittivities at high frequencies at ambient temperatures and above. An overall objective of electrical characterisation is to investigate the effects of composition and temperature on bulk permittivity, i.e. variation of bulk permittivity with composition and whether the permittivity varies, positively or negatively with temperature. Investigation of various possible sources of error and variations in permittivity measurement are therefore indispensable before a firm conclusion can be drawn in correlating permittivity with density, sintering temperature and electrodes. The electrical data were collected on samples whose sintering conditions have been optimised with respect to capacitance value, bismuth loss and pellet density. The focus of this paper is on the high temperature electri-

cal behaviour of optimised $Bi_3Zn_{1.84}Nb_3O_{13.84}$ via a systematic impedance spectroscopy study.

2. Experimental

Cubic pyrochlore $Bi_3Zn_{1.84}Nb_3O_{13.84}$ was prepared via conventional solid state reactions using Bi_2O_3, ZnO, and Nb_2O_5 as starting materials (all Alfa Aesar, 99.99%). ZnO and Nb_2O_5 were dried at 600 °C while Bi_2O_3 was dried at 300 °C, for 3 h prior to weighing. Stoichiometric quantities of the oxides were weighted and mixed with acetone in an agate mortar to ensure the homogeneity of the mixture. The resulting powder was transferred into a gold boat and pre-fired at 700 °C for 24 h (below Bi_2O_3 melting point of ca. 825 °C) in a Carbolite muffle furnace. Subsequently, the mixture was fired at 800 °C and 950 °C for 24 h with intermediate regrinding. The phase purity of the sample was examined at room temperature by X-ray diffraction using a Shimadzu X-ray powder diffractometer XRD-6000 equipped with a diffracted-beam graphite monochromator, with CuK_α radiation (1.5418×10^{-10} m). Pellets of a single phase sample were prepared using a stainless steel die measuring 8 mm in diameter. A sufficient amount of powder was added, cold pressed uniaxially, and sintered at 1050 °C in order to increase the mechanical strength and to reduce the intergranular resistance in the pellets. Gold paste (Engelhard) was smeared and hardened onto parallel faces of the ceramics.

The pellets with gold electrode attached were placed on a conductivity jig and inserted in a horizontal tube furnace. The pellets were characterised using an ac impedance analyser, Hewlett Packard LF HP4192A over the frequency range $5–1.3\times10^7$ Hz with the applied voltage of 100 mV. Conductivity measurements were carried out over the temperature range ca. 28–850 °C on heating and cooling cycles each at 50 °C interval. The samples were allowed to equilibrate at each temperature for 30 minutes prior to measurement. Most measurements were made in air, and where necessary in oxygen free nitrogen (OFN) at the flow rate of 80 cm^3/min for reducing atmosphere study. The nitrogen gas was supplied to a sealed tube furnace for 1 h in order to create a nitrogen atmosphere prior to measurement.

3. Results and discussion

Electrical properties of optimised $Bi_3Zn_{1.84}Nb_3O_{13.84}$ pellets with the density of ca. 90%, sintered at 1050 °C, were determined by ac impedance spectroscopy over the frequency range of 5 Hz–13 MHz in air. The measured impedance data are represented in the Nyquist form with a typical complex plane plot (Z'' vs Z'). The impedance is normalised by the geometric factor and represented in the form, $\rho^* = Z^*(S/d) = \rho' + j\rho''$ where ρ^* is the complex resistivity and S/d is the geometric factor. The parameters S and d represent the area and the separation of the electrodes [14, 15], re-

spectively. Perfect semicircles are only observed in the Cole–Cole plots of cubic pyrochlore $Bi_3Zn_{1.84}Nb_3O_{13.84}$ above 550 °C (Fig. 1).

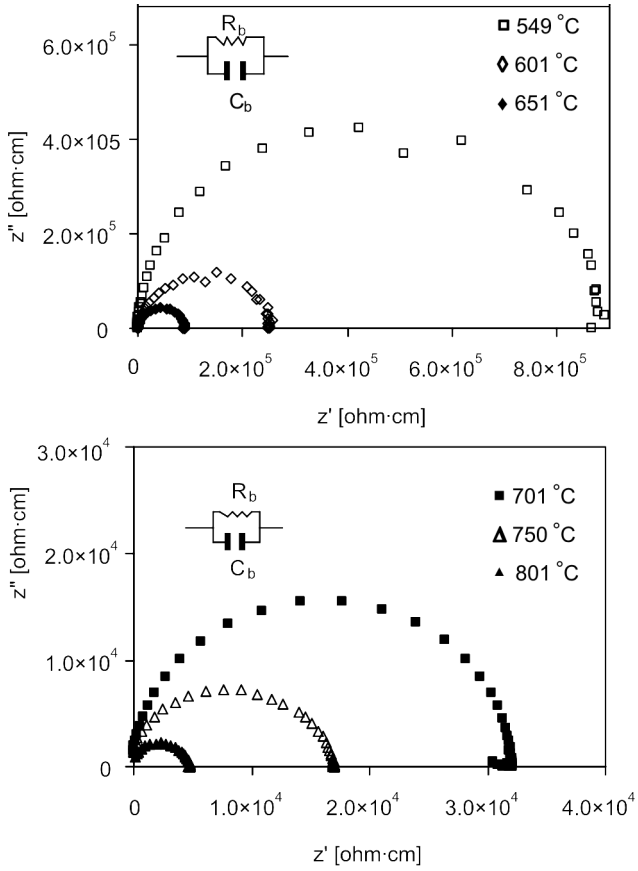

Fig. 1. Cole–Cole plots of $Bi_3Zn_{1.84}Nb_3O_{13.84}$ measured at various temperatures; $C_{max} = 1.19\times10^{-11}$ F·cm^{-1}

The impedance data can be represented by the equivalent circuit shown in the inset of Fig. 1. The circuit consists of parallel R and C elements of the bulk material and the total impedance Z^* for the circuit is given by:

$$Z^* = \frac{1}{j\omega C + \frac{1}{R}} = \frac{R}{1 + j\omega CR} = Z' - jZ'' \tag{1}$$

An associated capacitance of 1.19×10^{-11} F·cm^{-1} (after correction for jig) is obtained at 549 °C and this corresponds to the bulk properties of the material. The corresponding bulk resistivities, R_b of ca. 8.3×10^5 to ca. 2×10^3 Ω·cm over the temperature range 550–850 °C are obtained from the intercept on the real part of impedance. This

could be associated with the increase in thermally activated drift mobility of electric charge carriers according to the hopping conduction mechanism. In addition, the resistivity falls as the temperature increases, because the probability of carriers being promoted into the conduction band, or being transferred from one defect to another is governed by thermal fluctuations described by the Boltzmann statistics [16]. On the other hand, higher dielectric polarisation may result in higher electric permittivities and higher dielectric losses as the temperature increases [17].

For a highly resistive material, the Nyquist diagram is not completely defined as the data fitting may lead to a gross error. Hence, the capacitance and permittivity value can be extracted based on the electrical response in a high frequency range 10^5–10^7 Hz using the equation $-Z'' = 1/(jC_b \times 2\pi f)$ where Z'' is the imaginary part of impedance, $j = (-1)^{1/2}$ and ω is the angular frequency. The capacitance C_b of the bulk material can be determined from the slope of the plot $-Z''$ vs. $1/2\pi f$. A bulk capacitance of 1.19×10^{-11} F·cm^{-1} (after correction for stray capacitance from the empty jig) is obtained for $Bi_3Zn_{1.84}Nb_3O_{13.84}$ at 549 °C (Fig. 2) which agrees reasonably well with that obtained from the Cole–Cole plot ($\omega RC_b = 1$).

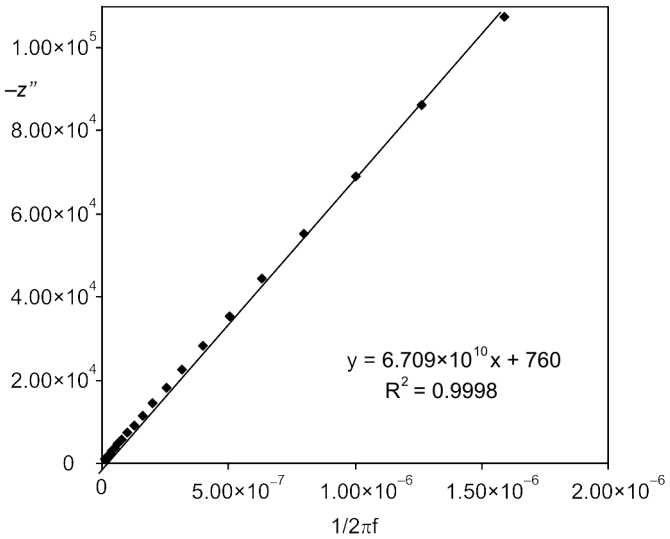

Fig. 2. Imaginary part of impedance, Z'' as a function of the reciprocal angular frequency at 549 °C

The impedance data of the material are further examined using the combined spectroscopic plots of imaginary components of the complex impedance, Z'' and electric modulus, M''. The frequency maxima of Z'' and M'' should be coincident, and the full width at half maximum (FWHM) should be equal to 1.14 decades for an ideal Debye response representing bulk properties. There appears to be no grain boundary effect as two overlapping peaks with FWHM value of ca. 1.15 decades are obtained (Fig. 3), indicating that the material is homogeneous.

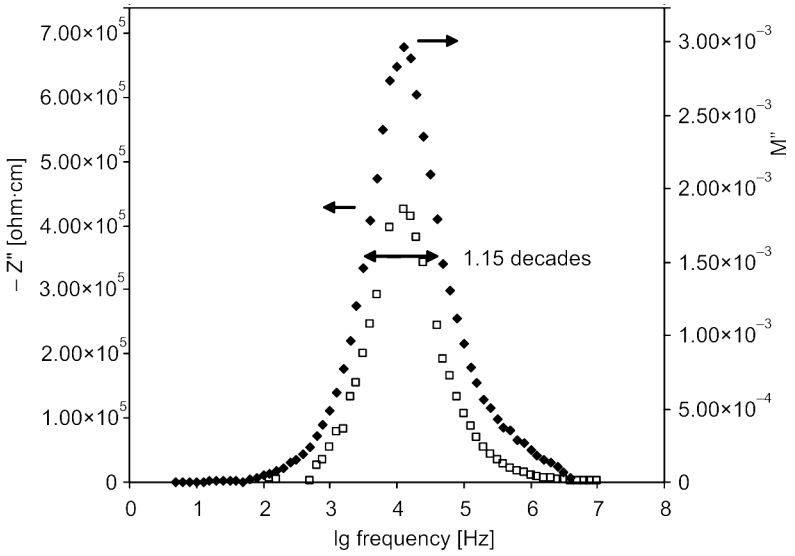

Fig. 3. Combined Z'' and M'' spectroscopic plots for cubic pyrochlore $Bi_3Zn_{1.84}Nb_3O_{13.84}$ at 549 °C

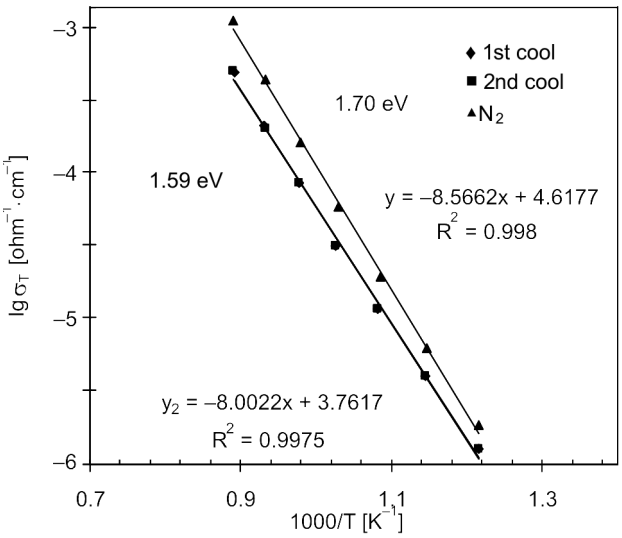

Fig. 4. Conductivity Arrhenius plots of cubic pyrochlore, $Bi_3Zn_{1.84}Nb_3O_{13.84}$

Figure 4 shows the electrical conductivity of the material as a function of temperature. The Arrhenius law is applied in order to correlate the observed behaviour with a general relation, $\sigma = \sigma_0 \exp(-E_a/kT)$ where σ_0 represents a pre-exponential factor, E_a is the apparent activation energy of the conduction process, k is Boltzmann's constant and T is the absolute temperature. The conductivity data are reproducible and reversible in heat–cool cycles with a high activation energy of ca. 1.59 eV. Usually, high

activation energy is required for the occurrence of a hopping type electronic mechanism, especially with the presence of defects of the oxygen vacancy in the pyrochlore structure [14, 15]. The conductivity at room temperature is determined by data extrapolation. Cubic pyrochlore, $Bi_3Zn_{1.84}Nb_3O_{13.84}$, exhibits conductivity which is an order of magnitude lower than that of bismuth zinc antimonite (BZS) material with the value of $1\times10^{-21}\ \Omega^{-1}\cdot cm^{-1}$ at room temperature. The high resistivity of Bi based pyrochlores has been noted in literature and these materials are mainly used for dielectric applications [18].

Oxides are susceptible to oxygen loss with creation of anion vacancies and associated reduction at high temperature, especially under reducing atmosphere where a process, $2O^{2-} \rightarrow O_2 + 4e^-$ takes place. In a nitrogen atmosphere, $Bi_3Zn_{1.84}Nb_3O_{13.84}$ exhibits n-type conduction behaviour with higher conductivity and the activation energy of 1.70 eV (Fig. 4). This may be considered as evidence that cation disordered pyrochlores (A ↔ B exchange) exhibit a high level of intrinsic oxygen Frenkel disorder (48*f* → 8*b*). It was suggested by Clayton et al. [19] that $Bi_3Zn_2Nb_3O_{14}$ pyrochlore disclosed an n- to p-type behaviour as a function of temperature and partial pressure of oxygen. The p-type conductivity dominated at high pressure of oxygen, under oxidizing conditions and n-type conductivity dominated at low p_{O_2} with considerable ionic contribution to the conductivity, due to the presence of the shallow minimum in conductivity measurements.

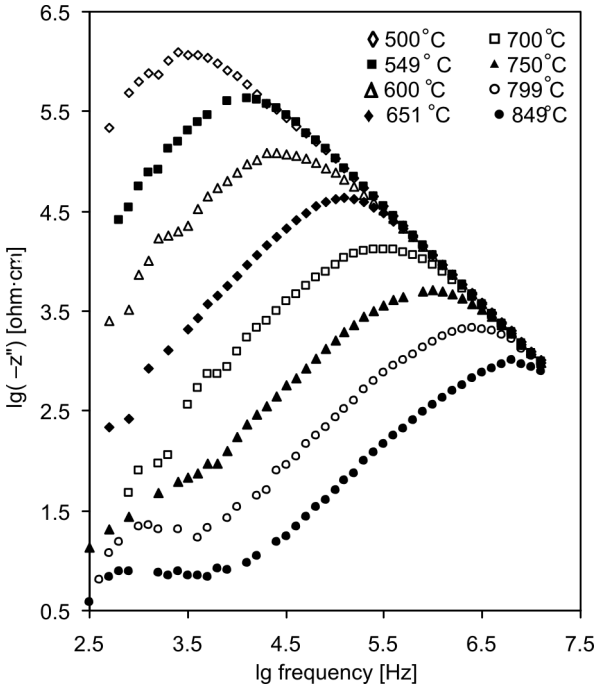

Fig. 5. Imaginary part of impedance as a function of frequency for cubic pyrochlore, $Bi_3Zn_{1.84}Nb_3O_{13.84}$ at various temperatures

A dispersion of imaginary impedance, Z'' as a function of frequency is shown in Fig. 5. The maxima of the curves shift towards a higher frequency region as the measuring temperature increases; this indicates the presence of a polarisation process in the dielectric material.

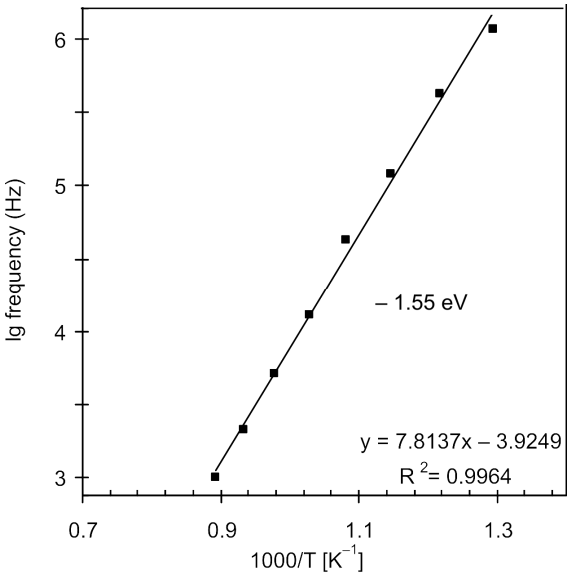

Fig. 6. Arrhenius plot for peak frequency of cubic pyrochlore, $Bi_3Zn_{1.84}Nb_3O_{13.84}$

Peak frequencies in Fig. 6 are used in the Arrhenius plot (peak frequency type) to show its dependence on temperature. Figure 6 shows the evolution of the peak frequency that follows the Arrhenius law with an apparent activation energy of 1.55 eV. This value is in good agreement with the activation energy calculated from the conductivity Arrhenius plot, i.e. 1.59 eV. This suggests strongly that the electrical behaviour of cubic pyrochlore, $Bi_3Zn_{1.84}Nb_3O_{13.84}$ is influenced by the polarisation phenomenon in the crystalline lattice and that the conduction mechanism is of the hopping type [14, 15].

The electric modulus is inversely proportional to the capacitance C. The peak heights of the modulus plots (Fig. 7) are independent of temperature, indicating that $Bi_3Zn_{1.84}Nb_3O_{13.84}$ does not exhibit ferroelectric properties in the temperature range studied. Similarly, the dielectric relaxation behaviour of ideal BZN cubic pyrochlore, $Bi_3Zn_2Nb_3O_{14}$ has been studied and it was suggested that the material is neither a dipolar glass nor a relaxor ferroelectric [20]. The complex dielectric response of $Bi_3Zn_2Nb_3O_{14}$ between 100 Hz and 100 kHz revealed a dielectric relaxation below the polar phonon frequencies. Relaxation at room temperature was observed at the frequency of 10^8 Hz, and the high frequency limit of relaxation frequencies was nearly temperature independent. The relaxation was postulated to be associated with hopping

of disordered Bi and Zn atoms at A sites (each of the A atoms occupy one of 6 equivalent, closely spaced positions) and hopping of O′ atoms among 12 sites [20].

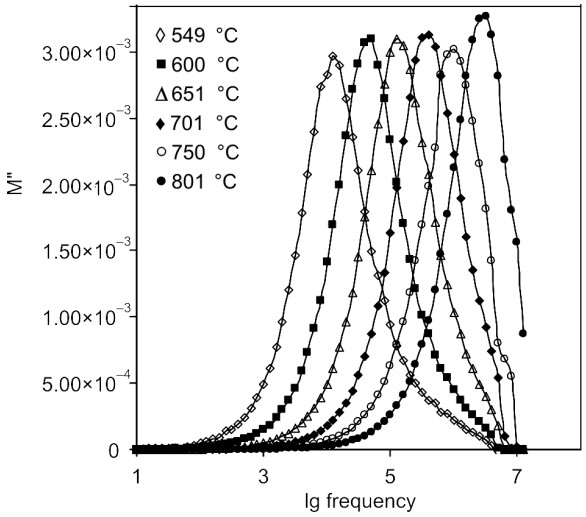

Fig. 7. Imaginary part of electrical modulus as a function of frequency

The complex electric permittivity ε^* can be expressed as a complex number

$$\varepsilon^* = \varepsilon'(\omega) - j\varepsilon''(\omega) \tag{2}$$

where ε' and ε'' are the real and imaginary parts of the complex permittivity.

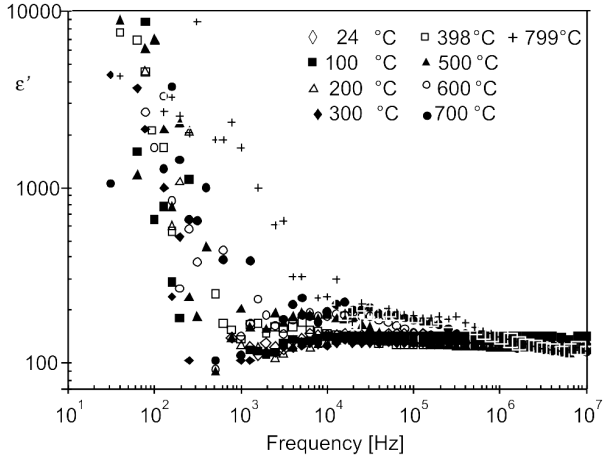

Fig. 8. Permittivity, ε', as a function of frequency at various temperatures

Figure 8 illustrates the relative permittivity of $Bi_3Zn_{1.84}Nb_3O_{13.84}$ as a function of frequency. High dispersion characteristics in the curves at frequencies lower than

1 kHz could be attributed to the dielectric material behaviour where a conduction mechanism of the hopping type is present [14, 15]. This is probably due to the atomic defects in cubic pyrochlores where intrinsic oxygen vacancies are present. On the other hand, permittivity depends on the concentration of defects and on the extent to which the internal field is raised above the applied field. Occurrence of a continuous flow of the current rather than a limited oscillation between sites is noted to be due to high concentration of defects and/or high probability of hopping events. This contribution to the permittivity is small while the resistivity remains at a sufficiently high level for the dielectric to be of practical interest [16]. The degree of dispersion decreases as the frequency increases. In the frequency range of 10–10^3 kHz, a frequency-independent response is observed over the entire temperature range studied (Fig. 8). This may be attributed to the inherent characteristic of dielectric materials as the oscillating system cannot follow the resonant frequency or jumping frequency, ω_r, in an applied field.

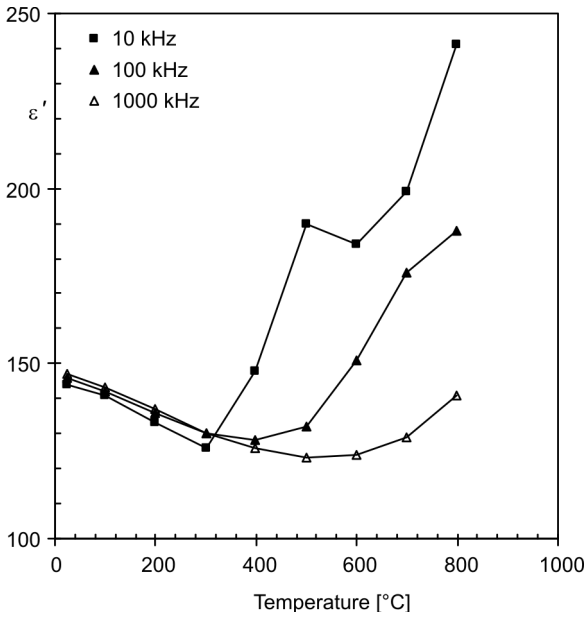

Fig. 9. Real part of complex permittivity
as a function of temperature at several frequencies

Figure 9 illustrates the temperature dependence of the real part of the complex permittivity at several frequencies. The decline in permittivity in the temperature range 25–400 °C (100–1000 kHz) indicates a negative temperature coefficient of permittivity of ca. 396 ppm/°C which is comparable to the reported value –400 ppm/°C [21, 22].

The dielectric loss can be expressed as

$$\tan\delta = \frac{\varepsilon''(\omega)}{\varepsilon'(\omega)} \tag{3}$$

A dense and pore free structure is a prerequisite for a low loss dielectric, as the pores may take up moisture which results in a higher dielectric loss, particularly if soluble ions are leached from the solid phase.

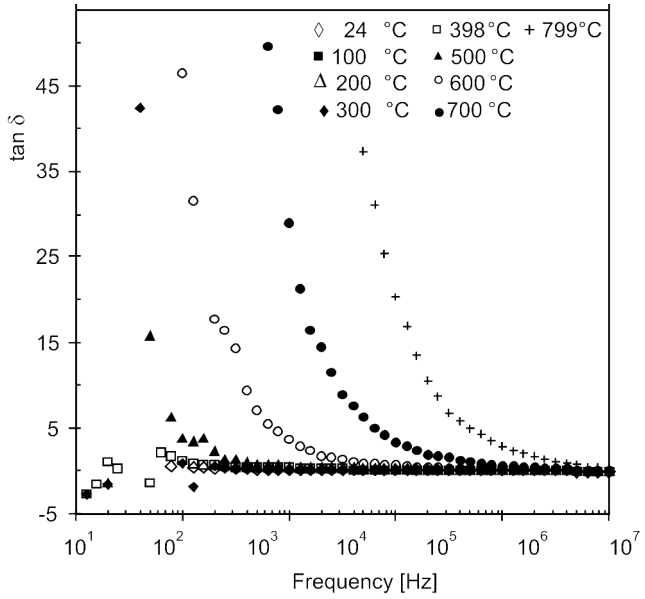

Fig. 10. Dielectric losses, tanδ, as a function of frequency at several temperatures

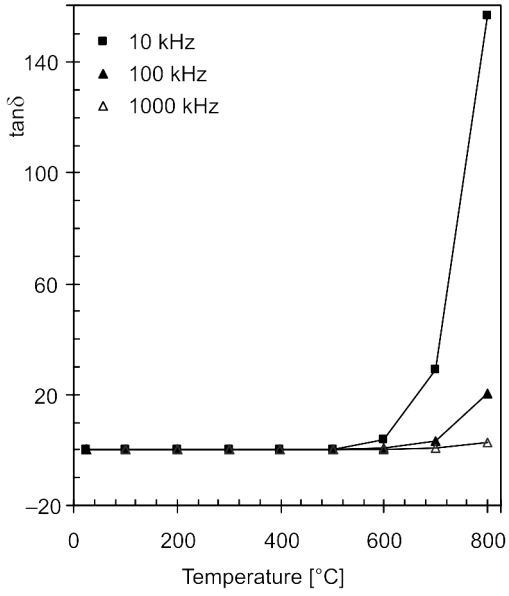

Fig. 11. Dielectric losses, tanδ, as a function of temperature at several frequencies

Dielectric losses at various temperatures are shown in Fig. 10. All the curves display a similar frequency independent behaviour below 500 °C. Above 500 °C, an appreciable increase in the dielectric losses is observed. Dielectric losses are strongly dependent on frequencies, i.e., lower losses are observed at higher frequencies (Fig. 11). The behaviour below 500 °C could be associated with the frequency independence of dielectric loss (above kilohertz region) of BZN cubic pyrochlore with hopping conduction mechanism mentioned earlier. High dielectric loss at low frequencies is possibly due to time availability for the displacement of defects. Energy is lost through the movement of the screening charge (adjustment of surrounding ions relative to their state when the defect is absent) against the applied field. The ratio of energy lost, W_L to energy stored, W_S in each hopping transition is represented by $W_L/W_S = (1 - \xi)/\xi$ where ξ is the restraint of screening imposed by the lattice [16]. On the other hand, increase in temperature (above 500 °C) may increase the number of thermally activated charge carriers (defects) and this will lead to displacement of defects. $Bi_3Zn_{1.84}Nb_3O_{13.84}$ possesses the highest value of relative permittivity and the lowest dielectric loss in comparison with two analogous systems, $Bi_3Zn_2M_3O_{14}$, (M = Ta and Sb). There is a decrease in the relative permittivity and increase in the dielectric loss going from Nb to Sb system with the values of ca. 148, 48 and 0.002, 0.006, respectively [22–24]. This could be associated with the substitution of less polarisable Sb^{5+} or Ta^{5+} cation.

4. Conclusion

The cubic pyrochlore, $Bi_3Zn_{1.84}Nb_3O_{13.84}$ exhibits a typical dielectric behaviour in the frequency and temperature ranges studied. High dispersion of permittivity and high dielectric loss at low frequencies, and frequency-independent permittivity and dielectric loss at high frequencies (> 100 kHz) with much lower permittivity and dielectric loss are observed. These phenomena could be attributed to the dielectric behaviour of the material, where a conduction mechanism of a hopping type is present. In general, the sample is highly resistive with a high activation energy of ca. 1.59 eV; a high relative permittivity value, 147 and low dielectric loss, 0.002, making it a potential candidate in multilayer ceramic capacitors.

Acknowledgements

Financial support from Ministry of Science, Technology and Innovation (MOSTI) is gratefully acknowledged. Special thanks are extended to Prof. A.R. West for his constructive suggestions and comments on impedance study.

References

[1] HEYWANG W., THOMANN H., *Positive Temperature Coefficient Resistors*, [In:] B.C.H Steele (Ed.), Electronic Ceramics, Elsevier, Amsterdam, 1991, p. 29.

[2] RAO C.N.R., GOPALAKRISHNAN J., *New Direction in Solid State Chemistry*, 2nd Ed., Cambridge University Press, Cambridge, 1997.
[3] MUKTHA B., DARRIET J., GIRIDHAR MADRAS., GURU ROW T.N., J. Solid State Chem., 179 (2006), 3919.
[4] SEGAL D.L., *Powders for Electronics*, [In:] B.C.H. Steele (Ed.), *Electronic Ceramics*, Elsevier, Amsterdam, 1991, p. 185.
[5] CANN D.P., RANDALL C.A., SHROUT T.R., Solid State Commun., 100 (1996), 529.
[6] ZHOU W., J. Solid State Chem., 101 (1992), 1.
[7] SUBRAMANIAM M.A., ARAVAMUDAN G., SUBBA RAO G.V., Progr. Solid State Chem., 15 (1983), 55.
[8] VALANT M., SURUROV J. Am. Ceram. Soc., 88 (2005), 2540.
[9] NINO J.C., LANAGAN M.T., RANDALL C.A., J. Mater. Res., 16 (2001), 1460.
[10] WITHERS R.L., WELBERRY T.R., LARSSON A-K., LIU Y., NOREN L., RUNDLOF H., BRINK F.J., J. Solid State Chem., 177 (2004), 231.
[11] TAN K.B., LEE C.K., ZAINAL Z., MILES G.C., WEST A.R., J. Mater. Chem., 15 (2005), 3501.
[12] VANDERAH T.A., LEVIN I., LUFASO M.W., Eur. J. Inorg. Chem., (2005), 2895.
[13] LEVIN I., AMOS T.G., VANDERAH T.A., RANDALL C.A., LANAGAN M.T., J. Solid State Chem., 168 (2002), 69.
[14] NOBRE M.A.L., LANFREDI S., Mater. Lett., 47 (2001), 362.
[15] NOBRE M.A.L., LANFREDI S., Appl. Phys. Lett., 81 (2002), 451.
[16] HERBERT J.M., *Ceramics Dielectrics and Capacitors*, [In:] D.S. Campbell (Ed.), *The Properties of Dielectrics*, Gordon and Breach, New York, 1985, p. 9.
[17] DU H.L., YAO .,X WANG H., Ferroelectrics, 262 (2001), 89.
[18] RANDALL C.A., NINO J.C., BAKER A., YOUN H-J., HITOMI A., THAYER R., EDGE L.E., SOGABE T., ANDERSON T.D., SHROUT T.R., TROLIER-MCKINSTRY S., LANAGAN M.T., Am. Ceram. Soc. Bull., (2003), 9101.
[19] CLAYTON J., TAKAMURA H., METZ R., TULLER H.L., WUENSCH B.J., J. Electroceramic, 7 (2001), 113.
[20] KAMBA S., POROKHONSKY V., PASHKIN A., BOVTUN V., PETZELT J., Phys. Rev. B., 66 (2002), 054106.
[21] NINO J.C., LANAGAN M.T., RANDALL C.A., J. Applied. Phys., 89 (2001), 4512.
[22] WANG X.L., WANG H., YAO .,X J. Am. Ceram. Soc., 80 (1997), 2745.
[23] YOUN H.J., SOGABE T., RANDALL C.A., SHROUT T.P., LANAGAN M.T., J. Am. Ceram. Soc., 84 (2001), 2557.
[24] DU H.L., YAO X., Mater. Electr., 15 (2004), 13.

Received 12 May 2008
Revised 31 October 2008